

Infrared laserinduced postpulse dissociation of CF₂HCl and CF₂Cl₂ under high pressure and fluence conditions

W. Strube, J. Wollbrandt, M. Rossberg, and E. Linke

Citation: *The Journal of Chemical Physics* **105**, 9478 (1996); doi: 10.1063/1.472781

View online: <http://dx.doi.org/10.1063/1.472781>

View Table of Contents: <http://scitation.aip.org/content/aip/journal/jcp/105/21?ver=pdfcov>

Published by the [AIP Publishing](#)

Articles you may be interested in

[Quasiclassical trajectory calculations for the OH\(X 2Π\) and OD\(X 2Π\)+HBr reactions: Energy partitioning and rate constants](#)

J. Chem. Phys. **105**, 9897 (1996); 10.1063/1.472855

[Coriolisdependent Stark effect of the 2ν₃ band of methane observed by saturated absorption spectroscopy](#)

J. Chem. Phys. **105**, 9027 (1996); 10.1063/1.472737

[Unimolecular decomposition of NO₃: The NO+O₂ threshold regime](#)

J. Chem. Phys. **105**, 6807 (1996); 10.1063/1.472527

[The highpressure range of the reaction of CH\(2Π\) with N₂](#)

J. Chem. Phys. **105**, 5423 (1996); 10.1063/1.472383

[Semiempirical MNDO, AM1, and PM3 direct dynamics trajectory studies of formaldehyde unimolecular dissociation](#)

J. Chem. Phys. **104**, 7882 (1996); 10.1063/1.471504



Infrared laser-induced post-pulse dissociation of CF₂HCl and CF₂Cl₂ under high pressure and fluence conditions

W. Strube, J. Wollbrandt, M. Rossberg, and E. Linke
Humboldt-Universität Berlin, Institut für Chemie, Forschungsgruppe Laser-Photochemie,
Rudower Chaussee 5, Haus 4.1, D 12484 Berlin, Germany

(Received 9 July 1996; accepted 29 August 1996)

The unimolecular decomposition of the halogenated methanes CF₂HCl (one main channel) and CF₂Cl₂ (two main channels) in the focused beam of a pulsed CO₂ laser under high pressure and fluence conditions ($p=100\text{ Pa}-2\text{ kPa}$; $\Phi=5-200\text{ J/cm}^2$) was studied by a special laser-induced fluorescence (LIF) technique, permitting spatially resolved fragment concentration measurements in the focal region. Considerable amounts of CF₂ product were formed *after* the end of the laser pulse. In the one-channel-dissociation case of CF₂HCl LIF measurements of the CF₂ yield distribution $Y(z,r)$ can be related to the spatial distribution of the average absorbed energy in the parent molecules. Only part of the absorbed energy is consumed by multiphoton dissociation, while most reactant molecules remain highly vibrationally excited in the focus volume far into the double cone. Using the long-lived CF₂ also as a probe for measuring the rotational, translational, and vibrational temperatures, the redistribution of the internal energy in the molecules and fragments involved is monitored. The post-pulse production of CF₂ is shown to be caused by the energy pooling $v-v$ transfer mechanism, while contributions of pyrolytic and gas dynamic processes are of little importance. © 1996 American Institute of Physics. [S0021-9606(96)01345-1]

INTRODUCTION

For a number of years ir lasers have been used as a versatile energy source in gas-phase chemistry for selective reactant activation.¹ Pressure and irradiation conditions chosen in practical applications, such as powder production,² isotope separation,³ or radical generation⁴ usually present a compromise between an acceptable yield and improved selectivity of the chemical reactions involved. While most fundamental studies are concerned with a detailed understanding of the primary photophysical and photochemical processes in infrared multiphoton excitation and decomposition under collision-free and/or low fluence (less than a few J/cm²) conditions,⁵ much less is known about the complex processes occurring in the high pressure/high fluence regime (pressure pulse length product $p \times \tau_p > 2 \times 10^5\text{ Pa ns}$, fluence $\Phi \geq 5\text{ J/cm}^2$), when using standard TEA lasers. This parameter range is of considerable importance. While the significant radical yields and subsequent radical reactions in this range are relevant to practical applications, the high excitation levels reached there can extend the underlying theoretical models. However, the laser-induced processes and their dependence on fluence and pressure are complex and difficult to predict in this range.

One of the phenomena observed under high pressure/high fluence conditions is the continued dissociation of the irradiated gas long after the end of the ir laser pulse, an effect which was found earlier for both substances studied in this paper. It was assumed to be originating from some collision-induced energy transfer (CF₂HCl,⁶ CF₂Cl₂⁷). A more detailed study is still missing and will be given in the present paper.

EXPERIMENT

The experiments involved real-time, *in situ* laser-induced fluorescence (LIF) detection of the \tilde{X}^1A_1 CF₂ produced in the ir multiphoton dissociation (IRMPD) of CF₂HCl



and of CF₂Cl₂



and in possible secondary reactions of the primary products of this latter two-channel unimolecular reaction having a fluence dependent branching ratio, which favors the CF₂Cl channel at high fluences.⁸

The experimental technique and apparatus were described previously.⁹ Briefly, the halomethanes were photolyzed with tightly focused ir radiation of a homemade pulsed CO₂ TEA laser operating in TEM₀₀ mode. The laser emission could be grating tuned to the respective absorption frequencies of the halomethanes [*9R*(32) at 1085.8 cm⁻¹ for CF₂HCl, *10P*(36) at 929.02 cm⁻¹ for CF₂Cl₂]. The typical CO₂-laser pulse shape consisted of a 350 ns (FWHM) main pulse containing approximately 50% of the energy, while the other 50% were contained in the pulse tail. In order to take into account the action of this tail, instead of a halfwidth or an effective pulse length τ the total pulse length $t_p = 2.9\text{ }\mu\text{s}$ is used throughout this paper. The laser beam was focused with an $f=8\text{ cm}$ lens. As a result, the Gaussian fluence field $\Phi(z,r)$ in the focal region was highly inhomogeneous [Fig. 5(b)] with a confocal parameter of 5 mm (twice the Rayleigh range) and a waist diameter $2w=190\text{ }\mu\text{m}$ ($1/e^2$ point).

The size of the stainless steel reaction cell was fitted to the irradiation conditions and the need to exclude wall effects (length 10 cm, diameter 3 cm). Gas flow rate (1.3 sccm at 800 Pa) and laser repetition rate (2 Hz) were adjusted to flush the probed region between laser shots. After checking the purity of the gases by ir absorption and gas chromatography they were then used without further purification. Pressures ranged between 100 and 2000 Pa. In some experiments argon was used as buffer gas at partial pressures up to 12 kPa.

The LIF technique used for determining the concentration of the photolysis fragments in real time is based on a frequency-doubled dye laser as probe [pulse duration 5.6 ns (FWHM), bandwidth 1.5 cm⁻¹]. After exciting with this laser an absorptive transition in the species to be detected, the measured signal is the fluorescence out of the electronically excited state, which is a measure of the concentration of that species in the selected rovibronic state in the electronic ground state. In order to monitor CF₂ it was usually excited from the vibronic level $v''=0$ of the ν_2 bending vibration in the electronic ground state \tilde{X}^1A_1 to the vibronic level $v'=2$ of the same vibration in its electronically excited state \tilde{A}^1B_1 . Individual rotational lines of CF₂ were not resolved. Vibrational temperatures of \tilde{X} CF₂ were determined by exciting it with the dye laser from the low-lying vibronic states $v''=0, 2, 3$ to a selected vibronic state ($v'=2$) in the \tilde{A} state, from which the fluorescence to the $v''=1$ state was measured. After corrections of the LIF signals for Franck–Condon factors and different saturation of the absorption transitions, the signals yield the relative population of the vibronic states and thus a vibrational temperature, provided the population follows a Boltzmann distribution. The saturation correction factors took into account the deviation of the LIF signal measured for a given dye laser energy E_{dl} from the linear LIF(E_{dl}) dependence. These deviations were determined in separate measurements, giving 53%, 40%, and 8% at the focus centre for $v''=0, 2, 3$, respectively, and for the standard dye laser energy of 20 μ J.

In order to improve spatial resolution and thus to probe regions of constant ir fluence, a collinear arrangement of the beams of CO₂ laser and dye laser was chosen. Furthermore, the dye laser was focused ($f=250$ mm) to a diameter ($1/e^2$) of 58 μ m, and the probed cylindrical volume was limited to 5.3×10^{-6} cm³ by reducing the height of the parallel monochromator slit (2 mm), onto which the fluorescence from that volume was imaged 1:1. Employing the spatially resolved fluorescence (SRF) technique,⁹ spatial concentration profiles of a given species could be measured in radial and/or axial scans by changing the relative focus position of the probe laser with respect to the photolysis laser focus, i.e., to the processing zone. Figure 1 shows typical radial SRF profiles taken at a fixed axial position. Timing between the two lasers was controlled with an analog delay generator at a jitter of 8.5 ns. The delay times t_d given for the dye laser refer to the onset of the CO₂ laser pulse. The fluorescence was detected by a photomultiplier tube (EMI 9558 QB, integration time constant 3 μ s), the signal of which was fed to a boxcar integrator with 400 ns gate.

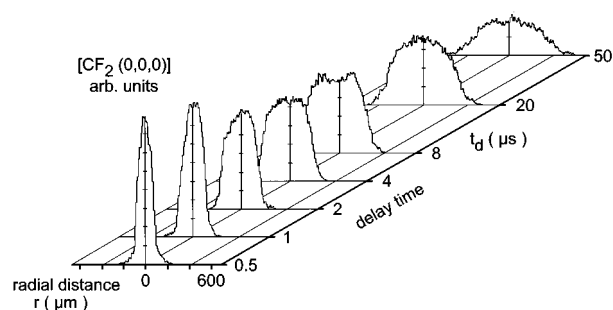


FIG. 1. CF₂ product concentration profiles obtained by radial scans at a fixed axial position ($z=0$).

The principal ability of our SRF arrangement to collect in a radial scan at a fixed axial position z all species of a given sort present at a given time in a region normal to the photolysis laser axis offers the unique possibility of determining the total amount $M(t)$ of that species in a volume of height h . For the given values of focal length f and slit height h this volume is approximately cylindrical in the focus core region studied. We thus can write

$$M(t) = 2\pi h \int_{r'=0}^{r'<R} C(r',t) r' dr' \quad (1)$$

with R being the cell radius. Since all parameters, such as vibrational temperature, rotational temperature, radiative lifetime, rates of formation, reaction and relaxation, obtainable by conventional LIF can be measured now for their spatial dependence, new information on processes occurring in the photolysis zone with its strong gradients is to be gained.

RESULTS

Post-pulse production of CF₂

Delaying the probe laser pulse with respect to the ir photolysis laser pulse yields the development in time of product concentration at a fixed location. Figure 2 shows such a

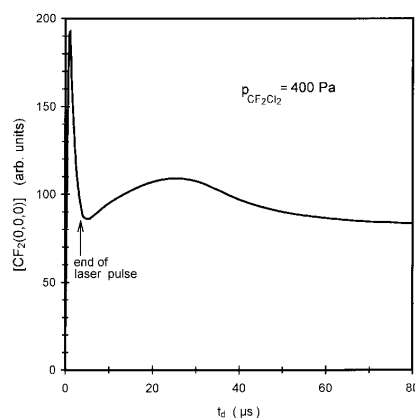


FIG. 2. Time-resolved fluorescence of CF₂ in the focus center ($z=0, r=0$). Maximum at 2 μ s by primary (photolytic) CF₂ formation; maximum at 25 μ s by secondary CF₂ formation.

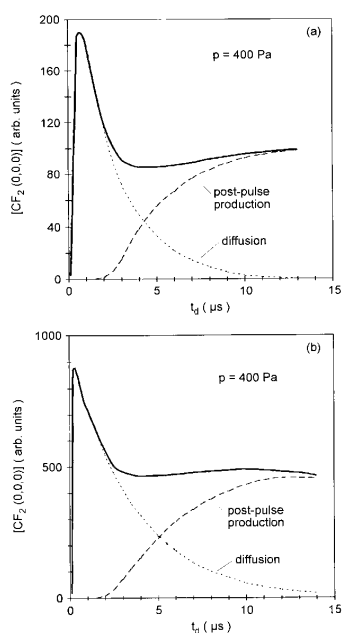


FIG. 3. Time-resolved LIF of CF_2 ($z=0$, $r=0$). Separation of the net LIF signal in a primary production and a post-pulse production part for the reactants CF_2Cl_2 (a) and CF_2HCl (b).

curve for CF_2 in its vibrational ground state in the centre ($z=0$, $r=0$) of the CO_2 laser focus. The main features of this curve are two consecutive maxima. As will be shown later, the first is caused by immediate photolytical fragmentation. The second is treated in the following.

The derivation of kinetic parameters from such measurements, however, is usually not straightforward due to the interference with reaction, relaxation, and diffusion of the species out of the probed region. In the present case it was possible to separate the contribution of diffusion, because (i) a similar curve for $\tilde{X}\text{CF}_2(0,3,0)$ showed that vibrational relaxation is much slower than diffusion, and (ii) the CF_2 density decay of the photolytically generated CF_2 could be fitted with an expression derived in Ref. 10

$$C(r,t) = \frac{C(t=0)}{2Dt} \int_0^{\rho_0} r \exp\left(\frac{-r^2}{4Dt}\right) \times \int_0^{r_0} r' \exp\left(\frac{-r'^2}{4Dt}\right) I_0\left(\frac{rr'}{2Dt}\right) dr' dr \quad (2)$$

for the diffusion out of the probe laser beam, the diffusion constant of which was found to be only dependent on pressure, not on fluence (ρ_0 and r_0 are the radii of the probe and photolysis laser beams, respectively; I_0 is the modified Bessel function of the first kind of order zero). Hence, the fraction of the photolytically generated, radially diffusing CF_2 could be subtracted from the measured signal. The residual signal [Fig. 3(a)] due to essentially post-pulse production of CF_2 in secondary processes then explains the second maximum in Fig. 2 at about $25 \mu\text{s}$ for the given pressure.

A qualitatively similar result is obtained for CF_2HCl [Fig. 3(b)]. Here, since IRMPD proceeds via only one chan-

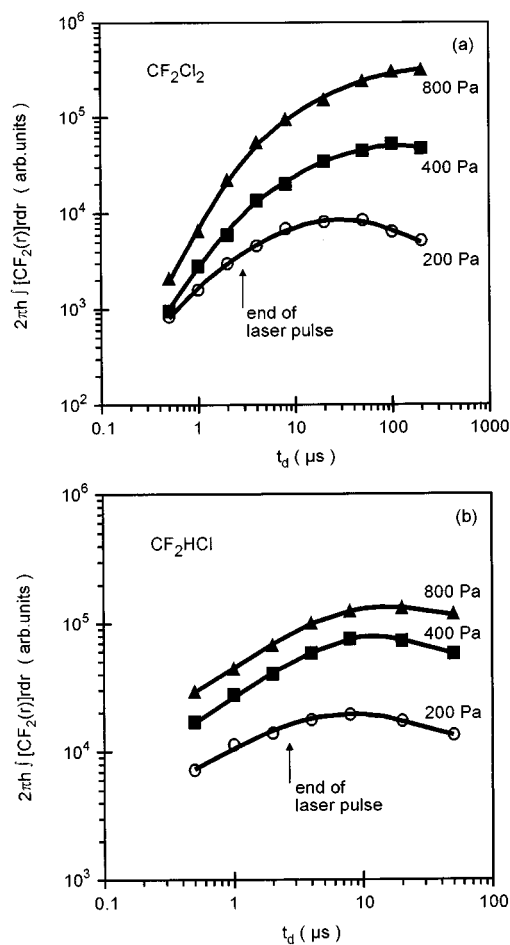


FIG. 4. The number of $\text{CF}_2(0,0,0)$ radicals $2\pi hf [\text{CF}_2(r)]rdr$ vs time at $z=0$ shows retardation of secondary CF_2 formation with reactant pressure (signals corrected for fluorescence quenching). (a) Reactant CF_2Cl_2 . (b) Reactant CF_2HCl .

nel leading directly to CF_2 , the yield and primary formation rate are higher, while the initial rate of secondary CF_2 formation is comparable to the CF_2Cl_2 case at the same pressures. This suggests a common, collision-controlled mechanism.

The effects of diffusion can, however, be completely eliminated by the integration procedure [Eq. (1)] given in the experimental section, which permits to cover all CF_2 radicals at any radial position at a given time. Integrating the radial concentration profiles measured for different times yields the curves shown in Fig. 4(a). As can be seen, the amount of CF_2 produced after the end of the laser pulse reaches multiples of the photolytically produced CF_2 . When the pressure is increased, the position of the curve maximum resulting from the combined action of $\text{CF}_2(0,0,0)$ formation and reaction to other products is shifted towards longer times. Relaxation of CF_2 from higher vibrational states also affects the position of the maximum.¹¹ Again, the CF_2 produced from CF_2HCl shows a qualitatively similar behavior [Fig. 4(b)], but the effect is less pronounced. Here, the factor for the post-pulse increase of CF_2 is independent of pressure.

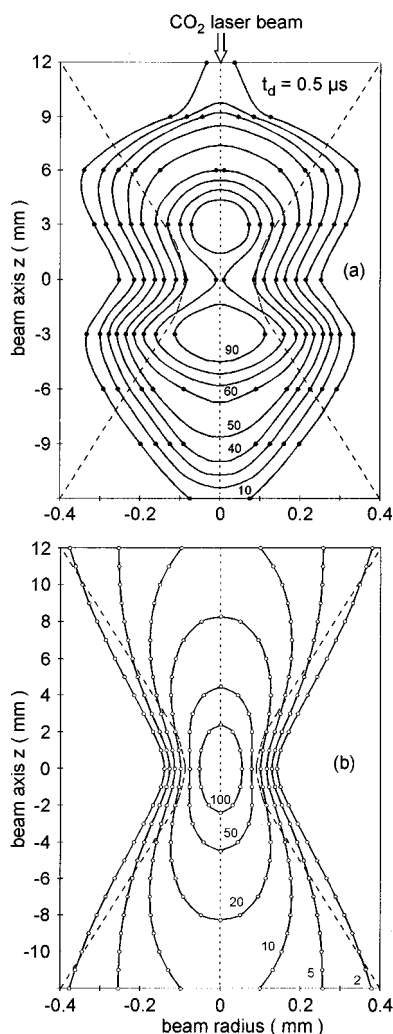


FIG. 5. (a) Lines of equal CF₂(0,0,0) fragment concentration (● measured values) for the reactant CF₂HCl. The numbers refer to percent of maximum value. (b) Focus of the CO₂ laser beam (without gas absorption). Lines of equal fluence are given as multiples of the fluence at the focusing lens. The broken curves $\Phi = \Phi(z, r=0)/e^2$ give an orientation for comparison with (a).

Inhomogeneous energy absorption

Due to the fluence dependence of the absorption cross section σ in the IRMPD of the parent molecules the inhomogeneous irradiation of a focused laser results in a spatially dependent energy absorption, i.e., in a spatially inhomogeneous dissociation yield. The spatial CF₂ yield distribution was obtained from radial LIF profiles measured at different axial positions (for a given time) by connecting points of equal LIF intensity. These represent lines of equal CF₂ concentration in a given quantum state. Figure 5(a) shows such an isoconcentration representation for a delay time $t_d = 500$ ns after the onset of the CO₂-laser pulse. The “altitude lines” give the fractional dissociation yield in percent of the maximum value, which corresponds to 20% of the total reactant concentration. This value was determined using the method given in Ref. 12 based on benzene as an emitter of known density and LIF characteristics.

As can be seen, the shape of the yield distribution is essentially determined by the characteristic fluence distribution $\Phi(z, r)$ shown in the equifluence line plot [Fig. 5(b)]. This distribution was calculated for the case of no absorption; it would yield a maximum fluence of 100 J/cm². However, a numerical calculation starting with a reasonable σ value at the entrance window and testing various $\sigma(\Phi)$ dependences, which would reproduce the average energy absorbed along the length of the cell, gave no significant changes of this fluence field (<10%). This is due to the relatively high total transmission value (>50%) and thus the small incremental changes $\Delta E(z)$ of the absorbed energy, so that $\Phi(z, r)$ is essentially determined by the respective beam cross section $\pi[w(z)]^2$.

In Fig. 5(a) the small axial deviation of the yield distribution from the fluence distribution is caused by absorption of the counterpropagating CO₂ and dye laser beams, respectively, along the length of the cell. The radial perturbation, however, is due to outward expansion, the velocity of which is dependent on z . Peak velocities of several hundred m/s were observed. The decrease of the CF₂ concentration to be seen in the very focus center is assumed to be due to probe-laser induced photolysis of the hot CF₂ precursor/parent molecule.¹³ Despite these minor distortion effects the observed decomposition pattern qualitatively reflects the energy absorption from the ir laser field, which is the source of all secondary post-pulse processes. Lack of a unique $\sigma(\Phi)$ relation prevents a quantitative $\langle E_{\text{abs}}(z, r) \rangle$ picture¹⁴ via $\langle E_{\text{abs}} \rangle = \Phi \times \sigma(\Phi)$, where $\langle E_{\text{abs}} \rangle$ is the average absorbed energy per molecule.

Energy transfer processes

As an average value $\langle E_{\text{abs}} \rangle$ defines only the “center of gravity,” not the width and shape of the vibrational energy distribution in the ensemble of parent molecules. Generally, the energy distribution is determined by the dynamics of the excitation processes. Hence, an explanation of the energy absorption at high halomethane pressures must include not only the fluence $\Phi(t) = \int_0^t I(t') dt'$, but also processes redistributing the molecular energy. The excitation level $\langle E_{\text{abs}} \rangle$ is given by the equilibrium of the optical pumping rate with the rates of dissociation and deactivation. Under the given high pressure conditions deactivation occurs essentially by collisions. At low excitation levels collisional energy transfer is relatively well understood both experimentally and theoretically.¹⁵ Especially for larger polyatomics, however, knowledge in the high excitation region is still only fragmentary.¹⁶

In order to gain some insight into the energy transfer processes involved here, the internal energy of the CF₂ product will be used as a probe, provided that—at least at some later time—its rotational and vibrational energies are essentially determined by exchange with its collision partners rather than by the partitioning of the reactant energy in the IRMPD process. This situation will have to be checked separately for rotational and vibrational energy transfer. Especially favorable conditions should exist for the $v-v$ transfer

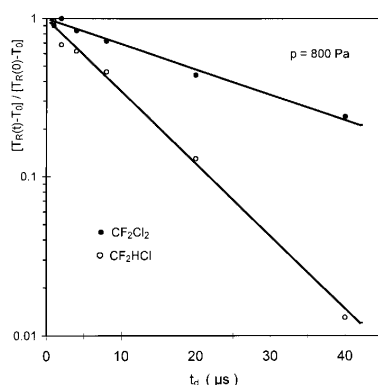


FIG. 6. Fit of the solution $T_R(t) - T_0 = (T_R(0) - T_0)\exp(-k_R m t)$ to the measured change of rotational temperature $T_R(t)$ with time (T_0 —room temperature).

between parent molecule and CF_2 , since the energy defect ΔE lowering the transfer rate by a factor f per $\Delta E \approx 300 \text{ cm}^{-1}$ ($f = 0.1 \times \text{collision rate}$)¹⁷ is less than 10 cm^{-1} even for cold parents and product [$\nu_8(\text{CF}_2\text{HCl}) = 1116 \text{ cm}^{-1}$ vs $\nu_3(\text{CF}_2) = 1112 \text{ cm}^{-1}$; $\nu_6(\text{CF}_2\text{Cl}_2) = 672 \text{ cm}^{-1}$ vs $\nu_2(\text{CF}_2) = 672 \text{ cm}^{-1}$]. Furthermore, the $v-v$ transfer rate k_{vv} between the freon molecules (number of vibrational degrees of freedom $s_i = 9$) and CF_2 should be lower only by a factor of 2 as compared to the transfer between parent molecules, since

$$k_{vv} \propto Z \frac{s_i s_j}{s_i + s_j} \quad (3)$$

with Z the gas kinetic collision rate.¹⁸ CF_2 is also especially suited as a probe, since it is long lived and its rotational as well as vibrational energies can be monitored by LIF.

A rotational temperature of CF_2 could only be determined for times $\geq 1 \mu\text{s}$, (≥ 80 collisions at $p = 800 \text{ Pa}$), because only then a model spectrum calculated under the assumption of a Boltzmann distribution with a rotational temperature T_R could be matched to the measured excitation spectrum of a vibrational band. Extrapolation of our results (Fig. 6) to shorter times gives maximum temperatures of 1070 K for CF_2HCl and 880 K for CF_2Cl_2 , respectively. From this maximum value the rotational excitation decays at a rate $k_R = 3.3 \times 10^{11} \text{ cm}^3/(\text{mol s})$ for CF_2HCl and $1.1 \times 10^{11} \text{ cm}^3/(\text{mol s})$ for CF_2Cl_2 . This rate was determined from the solution

$$T_R(t) - T_0 = (T_R(0) - T_0)\exp(-k_R m t) \quad (4)$$

of the linear differential equation

$$\frac{dT_R}{dt} = -k_R m (T_R - T_0), \quad (5)$$

describing the relaxation process (see Fig. 6), where T_0 is room temperature and m is concentration in mol/cm^3 . This rate is orders of magnitude lower than the collision rate or the known relaxation rate for rotation/translation $k_{R/T} = 1.3 \times 10^{14} \text{ cm}^3/(\text{mol s})$ in argon.¹⁹ Since at the times and pressures considered the $R-T$ degrees of freedom are in equilib-

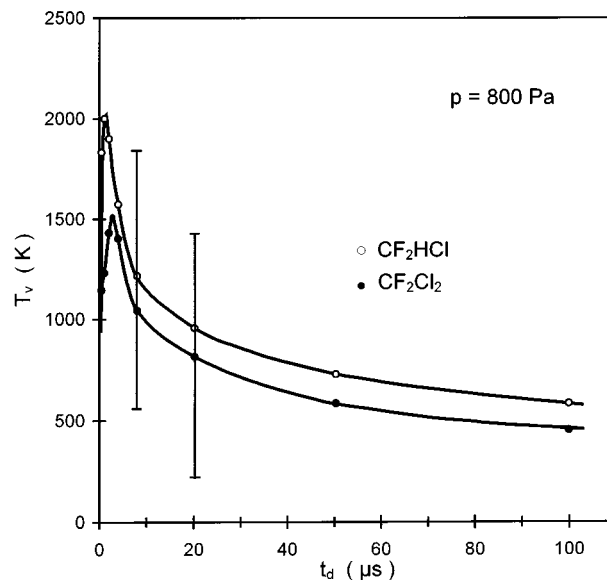


FIG. 7. Plot of the vibrational temperature vs time of the CF_2 product in the focus center ($z=0$, $r=0$).

rium, this extremely low value does not characterize the process of rotational relaxation in a cold buffer gas, but the slow cooling process of the gas heated by $v-T$ transfer from the freon molecules, which serve as a heat bath for the CF_2 fragments. At the given pressure, room temperature is reached in about $50 \mu\text{s}$.

The vibrational temperatures of the CF_2 product, however, show a different behavior. It was found that even for the shortest delay time $t_d = 500 \text{ ns}$ the population follows the Boltzmann law. Such a distribution was also found in Ref. 20 for nascent CF_2 in collision free IRMPD ($\Phi \leq 6 \text{ J}/\text{cm}^2$) of our reactants CF_2HCl ($T_v = 1160 \text{ K}$) and CF_2Cl_2 ($T_v = 1050 \text{ K}$). A plot of the vibrational temperatures of the CF_2 product vs time under our high fluence conditions (Fig. 7) shows not only that the observed maximum temperatures exceed these nascent temperatures, it also shows that this maximum excitation is only reached *after* the CO_2 laser pulse for the case of CF_2Cl_2 . Reducing the pressure by 50% yields this delay also for CF_2HCl . Obviously the measured vibrational energy distribution in the CF_2 product at the given pressure and fluence conditions must be the result of a fast and intense $v-v$ exchange with the undissociated and highly excited parent molecules. From the maximum value the vibrational temperature decays first at a rate of $(5 \pm 2) \times 10^{11} \text{ cm}^3/(\text{mol s})$, which is about the same as the cooling rate of the R/T temperature. While the latter temperature had reached room temperature after about $50 \mu\text{s}$, continued slowing down of the $v-T$ rate causes the establishment of thermal equilibrium, i.e., $T_v = T_{R/T}$, only after several hundred microseconds.

The radial T_v profiles in Fig. 8 show that already during the final part of the ir laser pulse the region of highly excited parent molecules/products stretches across a volume exceeding the CO_2 laser radius by several times. The long-lasting decay of the vibrational temperature of the CF_2 in space and time reflects the high energy content of the vibrational en-

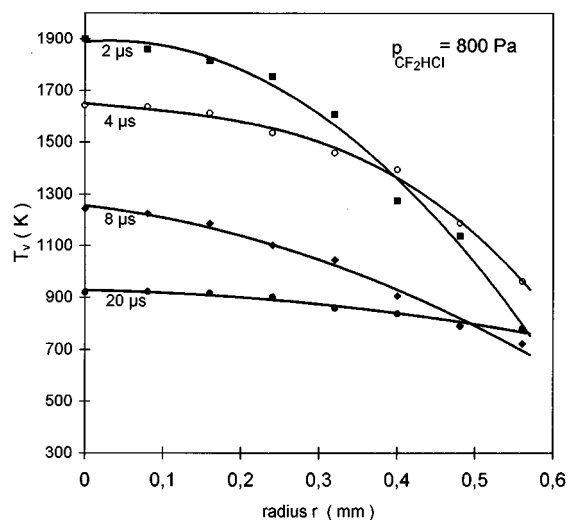


FIG. 8. Decay in space and time of the CF₂ vibrational temperatures.

ergy reservoir with which the CF₂ interacts. It is another clue to explain the delayed dissociation behavior.

It would be interesting to check now, if the high temperatures observed would explain the measured product yields on the grounds of a pyrolytic dissociation mechanism. For a thermal reaction the yield is only a function of temperature, not of the dynamics of reaching that temperature. We thus solve for the translational temperature of 1000 K the equation

$$\frac{d[\text{CF}_2]}{dt} = k_1[\text{CF}_2\text{HCl}] - k_2[\text{CF}_2]^2 - k_{-1}[\text{CF}_2][\text{HCl}] \quad (6)$$

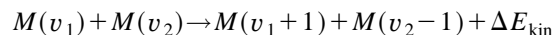
for the thermal CF₂ formation rate ($k_1 = 6.92 \times 10^{13} \exp(-233.5 \text{ kJ}/RT) \text{ s}^{-1}$,²¹ $k_2 = 1.3 \times 10^{11} (T/300)^{1/2} \exp(-5.0 \text{ kJ}/RT) \text{ cm}^3 \text{ mol}^{-1} \text{ s}^{-1}$,²² $k_{-1} = 2.14 \times 10^{11} \exp(-50.7 \text{ kJ}/RT) \text{ cm}^3 \text{ mol}^{-1} \text{ s}^{-1}$ ²³). Since in the beginning the bimolecular reaction terms are small with respect to the unimolecular decomposition term, this is straightforward. As a lower value one obtains a value of 60 ms to reduce the initial concentration of CF₂HCl to 50%, while the measured rate [see Fig. 3(b), 800 Pa] gives a time of 1.7 μs for reaching half the maximum concentration (net yield $Y \approx 0.5$). Thus primary CF₂ formation is essentially photolytic (IRMPD). As was shown above, the observed decay of the translation temperature within 50 μs also rules out significant contributions from a thermal dissociation mechanism for times longer than the CO₂ laser pulse length t_p .

DISCUSSION

The energy source responsible for the observed effects is the ir radiation contained in the CO₂ laser pulse of duration t_p . Upon multiphoton excitation of a resonant vibration of the molecule and subsequent fast intramolecular $v-v$ transfer high internal excitation levels or even unimolecular decomposition were achieved. The latter dissociation consumes part of the absorbed vibrational energy in a photolytically induced unimolecular IRMPD process with a correspond-

ingly high decomposition rate, which was detected as CF₂ formation rate. Large quantities of vibrational energy remain accumulated in the focal volume stretching far into the double cone of the focus. The molecular energy is then redistributed via different $v-X$ channels ($X=v, T$) during and especially after the input of radiative energy, resulting in the observed smearing out in time of product formation.

It was shown that $v-T$ energy transfer, despite causing translational temperatures as high as 1000 K, plays no role in producing significant amounts of CF₂ product. Accordingly, intermolecular $v-v$ transfer turns out to be the main redistribution route. So long as product concentrations are still low, $v-v$ transfer involves essentially the parent molecules themselves because of lack of other collision partners. From “cold” molecules in the focus neighborhood the excitation level is rising towards the focus center. Vibrational energy transfer of weakly excited molecules is relatively well understood (reviewed in Ref. 24). The main mechanism



is especially efficient (typically, 4–30 collisions) within the “ladder” of a respective vibration, owing to favorable resonance conditions in this quasiharmonic potential region. Upon higher excitation, i.e., with increasing anharmonicity the efficiency of this mechanism was found to drop. Thus it should not play a significant role at higher excitation levels. Whether this low-energy mechanism regains its role, however, when the quasicontinuum of vibrational states is reached, is still a matter of discussion.

Few studies exist so far on the $v-v$ energy transfer of highly excited freons (i.e., in the quasicontinuum), particularly of CF₂HCl and CF₂Cl₂. The limited number of experimental observables and the marked dependence of experimental results on the collision partners involved makes it difficult to establish models of general validity. Some trends, however, e.g., on the dependence of the average energy $\langle \Delta E \rangle$ transferred per collision on the excitation level, on the number of atoms in the colliding molecule/collision partner, or on temperature have been worked out:^{16,25}

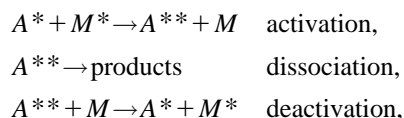
(i) $\langle \Delta E \rangle$ increases with $\langle E_{\text{abs}} \rangle$ of the excited species, showing a dependence between quadratic and linear; for more complex molecules (C₂-R, C₃-R) saturation was observed.

(ii) $\langle \Delta E \rangle$ increases with the number of atoms in the collision partner from about 5 kJ/mol (C₂H₄Cl₂ with He) to about 50 kJ/mol (C₂H₄Cl₂ with C₄H₈); for more complex partners the differences in transfer efficiencies are not pronounced. From data published for partners of comparable complexity to the freons studied here,²⁶ the transferred energies $\langle \Delta E \rangle$ should be somewhat greater than 15 kJ/mol, i.e., they should be in the energy range of the ir laser quanta.

(iii) $\langle \Delta E \rangle$ is only weakly dependent on temperature. In general, it decreases with rising temperature. Above a limiting temperature of about 1000 K, however, it increases due to the action of the repulsive part of the potential.

(iv) $v-v$ transfer is very efficient in establishing a Boltzmann distribution out of an originally arbitrary distribution.²⁷

Using these more or less general trends, notions can be developed of those processes, which eventually result in the observed high energy accumulation during the laser pulse and to the continued dissociation by energy redistribution after the pulse. Because of its energy dependence [cf. (i)] the energy exchange increases during the multiphoton absorption process, i.e., it is especially strong for energies close to the dissociation threshold D_0 . To describe schematically the effect of the energy transfer on MPA and MPD the following mechanisms are commonly used:



where A^* is the high vibrationally excited parent molecule ($E < D_0$), A^{**} is the overexcited parent molecule ($E > D_0$), and M is any collision partner (parent molecule, product, buffer gas). All these mechanisms are active both during and after the laser pulse.

Deactivation should play a major role in the course of the accumulation of vibrational energy in the irradiated species, because on the one hand, it makes less absorbers vanish by dissociation and on the other hand, it enhances absorption of desactivated molecules owing to their higher absorption cross section. The given *activation* mechanism must be of importance in the post-pulse vibrational relaxation processes responsible for collision-induced dissociation. It is called ‘energy pooling’²⁸ or ‘vibrational up-pumping’.²⁹ It starts from two ‘hot’ undissociated parent molecules, the separate vibrational energies of which are not sufficient for dissociation. Energy pooling means that the stored energy is now redistributed such that the sum of the vibrational energies of the colliding molecules and the relative kinetic energy along the line interconnecting their centres of gravity is exceeding the dissociation threshold D_0 within one molecule in the moment of closest approach. As a result of some energy transfer one of the partners gains a high enough energy to decompose with the unimolecular reaction rate $k(E)$.

Energy pooling has been shown to occur in a number of ir laser experiments at higher pressures. In Ref. 30 it was found responsible for continued spontaneous fluorescence of a product of CO_2 -laser irradiated SiF_4 at pressures in the range of a few Torr. In Ref. 31 the fluorescent product of the CO_2 -laser-induced dissociation of CDCl_3 at 1.3 kPa was identified by LIF to be CCl_2 . Post-pulse excitation of the electronically excited state responsible for this fluorescence required an energy equivalent to 17 ir laser quanta, i.e., the vibrational energy transferred during a collision may be much larger than collision-induced dipole selection rules would allow. While here contributions from the IRMPD product C_2Cl_4 , which was vibrationally hot due to absorption of ir radiation, could not be neglected, experiments with $\text{CH}_2\text{BrCH}_2\text{F}$, where none of the products showed absorption, yielded comparable results. Even for diatomics such as NO, collision-induced vibrational population of the $v''=15$ level from the $v''=1$ level excited by a cw CO laser at 12 kPa were

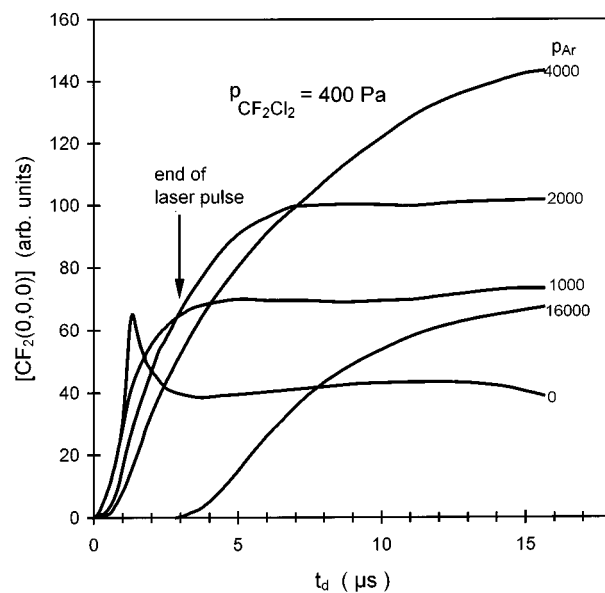


FIG. 9. The desactivating action of the buffer gas enhances absorption, i.e., storage of vibrational energy, which eventually causes unimolecular decay via ‘energy pooling.’

reported.³² This would correspond to a total energy transferred of $23\,300\text{ cm}^{-1}$.

Assuming (iv) to be fulfilled in our case, the ratio of activating to deactivating collisions can be given using the detailed balance of the transition probabilities P_{ij}, P_{ji} for the levels $E_i, E_j (E_i > E_j)$

$$\frac{P_{ji}}{P_{ij}} = \frac{\rho(E_i)}{\rho(E_j)} \exp[-(E_i - E_j)/kT]. \quad (7)$$

After calculation of the vibrational state densities $\rho(E)$ according to Whitten and Rabinovich,³³ for CF_2HCl a ratio $\rho(D_0)/\rho(D_0 - h\nu) = 1.58$ is found, where $h\nu$ is an ir quantum. The normalization condition $P_{ij} + P_{ji} = 1$ then yields a contribution for activating (dissociative) collisions of 34.9% for the acceptance of a quantum $\langle \Delta E \rangle = |E_i - E_j| = 1086\text{ cm}^{-1}$ (laser photon), if a vibrational temperature of 1500 K corresponding to an average number $\langle n \rangle = 10$ of absorbed laser photons is assumed. Since the density of states ratio becomes more favorable for lower energies, this percentage value gives a lower limit. According to (iii) the translational temperature should have no marked effect.

Hence, excited parent molecules of lower internal energy, which were shown to make up the majority of the molecules in the focus neighborhood far into the double cone, can be involved in unimolecular decay. Since this dissociation mechanism is collision-controlled, the measured net dissociation rate is orders of magnitude lower than the IRMPD rate, as can be seen from Fig. 3. The measured decay rate of the vibrational CF_2 temperature, which was much slower than the translational temperature evolution, reflects the high energy content of the vibrational energy reservoir with which it interacts.

The effect of an added inert buffer gas shown in Fig. 9 confirms the picture quite impressively. At a 40-fold buffer

gas surplus (16 000 Pa curve) dissociation can be completely suppressed during the ir laser pulse. Since no absorbers are lost, the total absorbed energy was increased by a factor of about 2. Subsequently, this stored vibrational energy is redistributed by $v-v$ energy pooling, yielding the dissociative action shown. A marked effect of $v-T$ processes can be ruled out due to the increased heat capacity (by 40 times).

The effect of a *radiative* heating of the CF₂ product, as it may occur at the wavelength chosen for IRMPD of CF₂HCl, could not be clarified. The lack of such a product resonance at the laser wavelength chosen is not the only reason, why results quantitatively different from CF₂HCl were obtained for the parent molecule CF₂Cl₂. Typical of CF₂Cl₂ is also the small primary production of CF₂, the respective molecular elimination channel is only of minor importance at high fluences (branching ratio <0.12 for $\Phi > 6$ J/cm²⁸). The initial CF₂ concentration being so low, the later increase is that marked, as was shown in Fig. 4(a). It can only be the result of secondary reactions.

Still controversial is the contribution of the secondary dissociation of the major primary product CF₂Cl, recombining to our major stable product 1,2-C₂F₄Cl₂. In Ref. 8 secondary dissociation of a fraction of 20% was estimated at a fluence of 6 J/cm² under molecular beam conditions. According to the results of this paper it is likely that under the present conditions an intense $v-v$ exchange with the hot parent molecules renders the fragment highly vibrationally excited, should the nascent CF₂Cl not already be hot due to energy partitioning in the IRMPD process. In any case, this situation would promote further vibrational heating by absorption of ir radiation, although the *linear* absorption band at 1149 cm⁻¹ is off-resonance from our laser wavelength. Then the situation is comparable to that for CF₂HCl, i.e., energy pooling explains the qualitatively similar results for CF₂Cl₂.

¹M. Quack, *Infrared Phys.* **29**, 441 (1989); *Lasers in Chemistry*, Special Issue of Proc. Indian Acad. Sci. (Chem. Sci.) **103**, 201 (1991); Proc. 2nd Conf. Lasers in Chemistry, Trieste (Italy), Nov. 1993.

²J. Förster, M. v. Hoesslin, and J. Uhlenbusch, *Appl. Phys. B* **62**, 609 (1996).

³J. Göthel, M. Ivanenko, P. Hering, W. Fuss, and K. L. Kompa, *Appl. Phys. B* **62**, 329 (1996).

⁴J. Wollbrandt, M. Rossberg, W. Strube, and E. Linke, *J. Mol. Spectros.* **76**, 385 (1996).

⁵Ber. Bunsenges, *Phys. Chem.* **99**, 231 (1995).

⁶K. Sugawara, A. Watanabe, Y. Koga, H. Takeo, K. Fukuda, J. Hiraishi, and Ch. Matsumura *J. Phys. Chem.* **93**, 3647 (1989).

⁷P. K. Chowdhury, Ber. Bunsenges, *Phys. Chem.* **95**, 1626 (1991).

⁸D. Krajnovich, F. Huisken, Z. Zhang, Y. R. Shen, and Y. T. Lee, *J. Chem. Phys.* **77**, 5977 (1982).

⁹W. Strube, J. Wollbrandt, M. Rossberg, and E. Linke, *Rev. Sci. Instrum.* **65**, 129 (1994).

¹⁰K. Reihls, Ph.D. thesis, University of Göttingen, 1989.

¹¹W. Strube, J. Wollbrandt, M. Rossberg, and E. Linke, in *Time-resolved Vibrational Spectroscopy*, edited by A. Lau, F. Siebert, and W. Werncke (Springer-Verlag, Berlin, 1994), p. 173.

¹²D. S. King, and J. C. Stephenson, *J. Am. Chem. Soc.* **100**, 7151 (1978).

¹³M. Rossberg, W. Strube, J. Wollbrandt, and E. Linke, *J. Photochem. Photobiol. A* **80**, 61 (1994).

¹⁴J. L. Lyman, S. D. Rockwood, and S. M. Freund, *J. Chem. Phys.* **67**, 4545 (1977).

¹⁵D. J. Krajnovich, C. Parmenter, and D. L. Catlett, *Chem. Rev.* **87**, 237 (1987).

¹⁶I. Oref and D. C. Tardy, *Chem. Rev.* **90**, 1407 (1990).

¹⁷J. D. McDonald, *Ann. Rev. Phys. Chem.* **30**, 29 (1979).

¹⁸V. N. Bagratashvili, V. N. Burimov, M. V. Kuz'min, and A. P. Sviridov, Preprint 3/1983 (Academy of Sciences, USSR, Troitsk, 1983).

¹⁹J. C. Stephenson, *J. Chem. Phys.* **70**, 4496 (1979).

²⁰D. S. King, *Adv. Chem. Phys.* **50**, 105 (1982).

²¹J. W. Edwards and P. A. Small, *Nature (London)* **202**, 1329 (1964).

²²K. P. Schug, Ph.D. thesis, University of Göttingen, 1976.

²³D. S. Y. Hsu, M. E. Umstead, and M. C. Lin, *ACS Symp. Series* **66**, 128 (1978).

²⁴G. W. Flynn, *Acc. Chem. Res.* **14**, 334 (1981).

²⁵H. Hippler and J. Troe, in *Advances in Gas-Phase Photochemistry and Kinetics*, edited by M. N. R. Ashfold and J. E. Baggott (Royal Society of Chemistry, London, 1989), Vol. 2, p. 209.

²⁶M. Quack and J. Troe, in *Gas Phase Kinetics and Energy Transfer*, edited by P. G. Ashmore and R. J. Donovan (A Specialist Periodical Report) (Chem. Soc., London, 1977), Vol. 2, p. 175.

²⁷C. D. Cantrell, S. M. Freund, and J. L. Lyman, in *Laser Handbook*, edited by M. L. Stitch (North Holland, Amsterdam, 1979), Vol. IIIb, p. 529.

²⁸I. Oref, *J. Chem. Phys.* **75**, 131 (1981).

²⁹G. A. McRae, A. B. Yamashita, and J. W. Goodale, *J. Chem. Phys.* **93**, 5997 (1990).

³⁰V. E. Merchant, *Opt. Commun.* **25**, 259 (1977).

³¹M. Ivanco, G. A. McRae, R. A. Back, J. W. Goodale, and P. E. Lee, *J. Chem. Phys.* **96**, 5191 (1992).

³²S. Saue, O. Schulz, W. Urban, I. Adamovich, M. J. Grassi, and J. W. Rich, *Verhandlungen Dt. Phys. Ges.* **3**, 362 (1993).

³³G. Z. Whitten and B. S. Rabinovitch, *J. Chem. Phys.* **38**, 2466 (1963).